Poly(ethylene terephthalate)/Polypropylene Microfibrillar Composites. III. Structural Development of Poly(ethylene terephthalate) Microfibers

F. K. P. Leung,[1] W. L. Cheung,[1] X. D. Lin,[2] D. Jia,[2] C. Y. Chung[3]

[1]*Department of Mechanical Engineering, University of Hong Kong, Hong Kong, People's Republic of China*
[2]*Department of Polymer Materials Science and Engineering, South China University of Technology, Guangzhou, People's Republic of China*
[3]*Department of Physics and Materials Science, City University of Hong Kong, Hong Kong, People's Republic of China*

Received 22 March 2006; accepted 22 March 2006
DOI 10.1002/app.24750
Published online in Wiley InterScience (www.interscience.wiley.com).

ABSTRACT: Poly(ethylene terephthalate) was extruded, solid-state-drawn, and annealed to simulate the structure of poly(ethylene terephthalate) microfibers in a poly(ethylene terephthalate)/polypropylene blend. Differential scanning calorimetry and wide-angle X-ray scattering analyses were conducted to study the structural development of the poly(ethylene terephthalate) extrudates at different processing stages. The as-extruded extrudate had a low crystallinity ($\sim$ 10%) and a generally random texture. After cold drawing, the extrudate exhibited a strong molecular alignment along the drawing direction, and there was a crystallinity gain of about 25% that was generally independent of the strain rates used (0.0167–1.67 s^{-1}). 2θ scans showed that the strain-induced crystals were less distinctive than those from melt crystallization. During drawing above the glass-transition temperature, the structural development was more dependent on the strain rate. At low strain rates, the extrudate was in a state of flow drawing. The resultant crystallinity hardly changed, and the texture remained generally random. At high strain rates, strain-induced crystallization occurred, and the crystallinity gain was similar to that in cold drawing. Thermally agitated short-range diffusion of the oriented crystalline molecules was possible, and the resultant crystal structure became more comparable to that from melt crystallization. Annealing around 200°C further increased the crystallinity of the drawn extrudates but had little effect on the texture. © 2007 Wiley Periodicals, Inc. J Appl Polym Sci 104: 137–146, 2007

Key words: annealing; blends; drawing; molecular dynamics

INTRODUCTION

In previous articles,[1,2] the morphological development of a 20/80 blend of poly(ethylene terephthalate) (PET) and polypropylene (PP) in melt extrusion and its solid-state drawing behavior are reported. Strain-induced crystallization of PET occurs, and its extent is a parameter of the drawing condition and draw ratio.[3,4] Drawing induces bundle crystals, which are oriented along the fiber axis. These crystals are highly stressed, less perfect, and smaller in size, and they will melt at a lower temperature than melt-crystallized crystals.[5] The kinetics of cold crystallization of preoriented PET yarns has been reported to change from three-dimensional to two-dimensional and finally one-dimensional rodlike growth with increasing molecular orientation.[6] Through wide-angle X-ray scattering (WAXS) analysis, molecules of drawn PET have been shown to align preferentially along the loading direction.[7–9]

In our overall study, solid-state-drawn PET/PP extrudates will be further processed by compression or injection molding to form the final parts. A typical molding temperature for the PP matrix is around 200°C. Although the molding temperature is below the melting point of PET, it is well above the glass-transition temperature (T_g). The oriented molecules in the drawn PET microfibers may relax or undergo further crystallization. Both phenomena will affect the properties of the microfibers and consequently the properties of the blend. In this work, pure PET extrudates were drawn under conditions similar to those of the PET/PP blend extrudates and then annealed to simulate the effects of solid-state drawing and subsequent molding processes on the structure of the PET microfibers. Differential scanning calorimetry (DSC) and WAXS analyses were performed to follow the structural development of the PET extrudates during the solid-state-drawing and annealing processes. The results will be used to assess the structure of the PET microfibers in the blend and for future investigations of the mechanical properties of the microfibrillar composites.

Correspondence to: W. L. Cheung (wlcheung@hkucc.hku.hk).

Contract grant sponsor: Hong Kong Research Grants Council (through a Competitive Earmarked Research Grant); contract grant number: HKU 7064/00E.

Journal of Applied Polymer Science, Vol. 104, 137–146 (2007)

EXPERIMENTAL

Melt extrusion, solid-state drawing, and annealing

The PET resin was dried at 120°C for 4 h before extrusion. The extruder setup has been described previously.[1] The temperature settings along the extruder barrel were T_1 (near the hopper) = 220°C, T_2 = 280°C, $T_3 = T_4$ = 300°C, and die temperature = 300°C. The screw rotational speed was 22 rpm, and the postextrusion hauling speed was 23 m/min. The extrudate was immediately quenched in a water channel after the die. The details of the solid-state drawing process have been reported earlier.[2] The distance between the clamps was 10 mm; therefore, the corresponding draw rate was 0.0167 s^{-1} for the minimum draw speed of 10 mm/min and 1.67 s^{-1} for the maximum draw speed of 1000 mm/min used in this study. Annealing was performed in an air-circulation oven under stress-free conditions.

Measurement of the crystallinity

The crystallinity of the PET samples before and after solid-state drawing and after annealing was determined by DSC. The details have been reported earlier.[2] The enthalpy of melting of crystalline PET was taken to be 140 J/g.[10]

WAXS

The WAXS experiments were performed on a Siemens D500 diffractometer (Munich, Germany). The Cu-anode X-ray generator was operated at 40 kV and 20 mA. The X-rays were filtered by a nickel filter. Sections of the drawn PET extrudates were lined up side by side on an acrylic plate and secured with 3M double-sided tape (St. Paul, MN) to form a monolayer specimen with an area of 25 × 25 mm^2. Trial tests were also conducted with Blu-Tak and other adhesive tapes, but they all showed diffraction peaks on the 2θ scan patterns and therefore were not used. 2θ scans were first performed to identify the diffraction peaks of both the as-extruded and drawn PET extrudates, and then pole figure analyses were carried out on the basis of the most distinctive peaks to investigate the textures of the extrudates. The pole figure analyses were performed in a reflection mode, and the test orientations of the sample were achieved with a goniometer. The software was Textan 3 (University of Manchester, UK) with a built-in background-correction function. A compression-molded PET plate was also analyzed with X-rays. The 1-mm-thick plate was molded at 300°C and air-cooled to attain high crystallinity. The surface of the PET plate was lightly polished with a piece of felt, washed with detergent, and finally rinsed in tap water to remove the mold-releasing agent and other contaminants before the analysis. The surface deformation of the sample caused by the polishing process was minimal, and it is believed that the molecular orientation was not significantly affected.

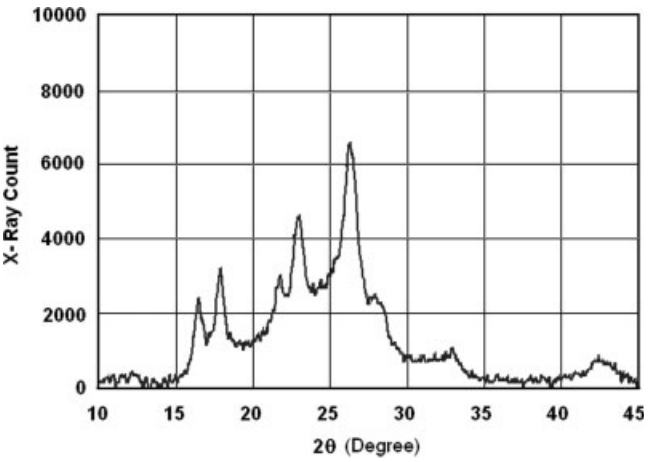

Figure 1 2θ scan pattern of a compression-molded PET plate.

RESULTS AND DISCUSSION

Structure of the PET extrudates

Because PET is the most commercially important polyester, its crystal structure has been intensively studied.[11–15] Within the triclinic crystal, the $(\bar{1}05)$ planes are roughly perpendicular to the chain axis, whereas the (100) planes are roughly parallel to the phenyl planes and the (010) planes are at 80 and 59° to the $(\bar{1}05)$ and (100) planes, respectively.[12] Figure 1 shows the 2θ scan pattern of the compression-molded PET plate, and the diffraction peaks at 16.3, 17.7, 21.8, 23.1, and 26.2° correspond to the $(0\bar{1}1)$, (010), $(\bar{1}11)$, $(\bar{1}10)$, and (100), planes, respectively.[5]

Figure 2(a–f) shows the typical 2θ scan patterns of PET extrudates drawn under different conditions, and that of the as-extruded sample is included for comparison. The diffraction pattern of the as-extruded sample resembles that of amorphous PET, and there is no distinctive diffraction peak. This is probably because of its low crystallinity (~ 10%). For extrudates cold-drawn at 10 mm/min [Fig. 2(a)], the increase in the diffraction intensity can be attributed to the higher crystallinity after drawing (Table I). Still, there is no distinctive peak, and this suggests that the strain-induced crystals were far from perfect. As the drawing speed was increased to 100 mm/min, two broad peaks gradually developed near 17.5 and 25° despite a similar crystallinity gain in comparison with the specimen drawn at 10 mm/min. For extrudates drawn at 50 and 70°C, the 2θ scan patterns [Fig. 2(b,c)] and crystallinity were generally similar to those of the cold-drawn samples, except that higher drawing speeds could be used without the samples being broken. The higher drawing temperatures probably facilitated the relaxation of some highly strained molecules and hence stabilized the growth of the neck.

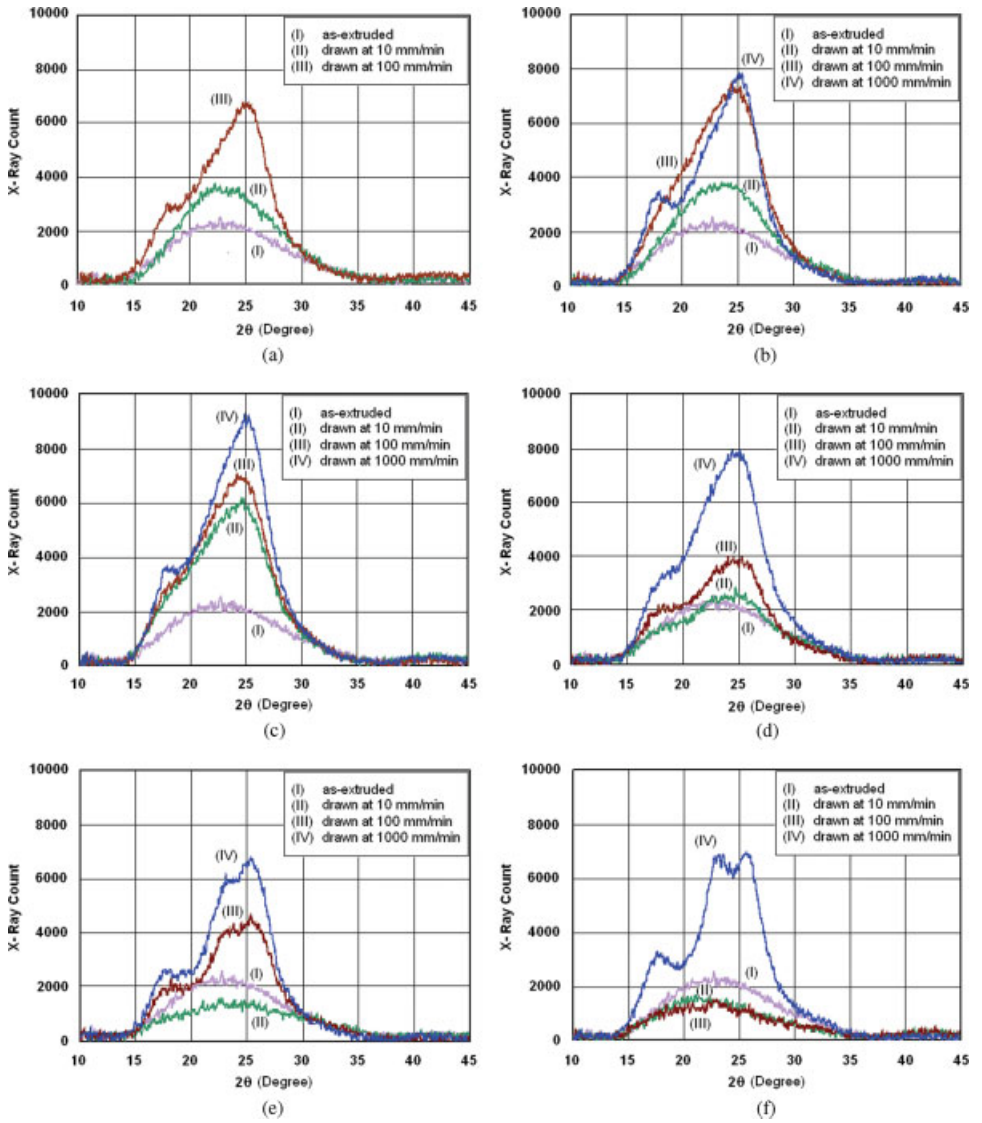

Figure 2 2θ scan patterns of PET extrudates (a) solid-state-drawn at 23°C, (b) drawn at 50°C, (c) drawn at 70°C, (d) drawn at 80°C, (e) drawn at 90°C, and (f) drawn at 100°C. [Color figure can be viewed in the online issue, which is available at www.interscience.wiley.com.]

During low-speed drawing below T_g, thermally agitated diffusion was restricted, and the tort molecular segments were largely aligned by the drawing force; this resulted in the formation of small, imperfect crystallites or paracrystals. The lattice constants of these paracrystals varied considerably, and this led to wide diffraction peaks. They overlapped each other and appeared as one single broad peak near 25° [Fig. 2(a–c)]. When drawing was performed at higher speeds, however, there was a significant temperature rise in the neck due to internal friction. Therefore, some short-range molecular diffusion was possible and gave rise to another diffraction peak near 17.5°.

TABLE I
Draw Ratio, Crystallinity, and Annealing (220°C) Shrinkage of Cold-Drawn PET Extrudates

Drawing speed (mm/min)		10	20	50	100	200
Draw ratio	1	3.6	3.8	4.4	5.0	5.3
Crystallinity (%)	10.3	35.3	36.5	36.2	36.4	37.3
Crystallinity after annealing for 10 min (%)	29.5	40.8	40.7	42.7	41.6	40.1
Crystallinity after annealing for 1 h (%)	35.2	45.2	47.3	47.4	48.3	45.8
Shrinkage after annealing for 10 min (%)	3.6	25.6	27.5	27.3	27.4	28.4
Shrinkage after annealing for 1 h (%)	3.6	24.0	27.9	27.3	30.0	27.4

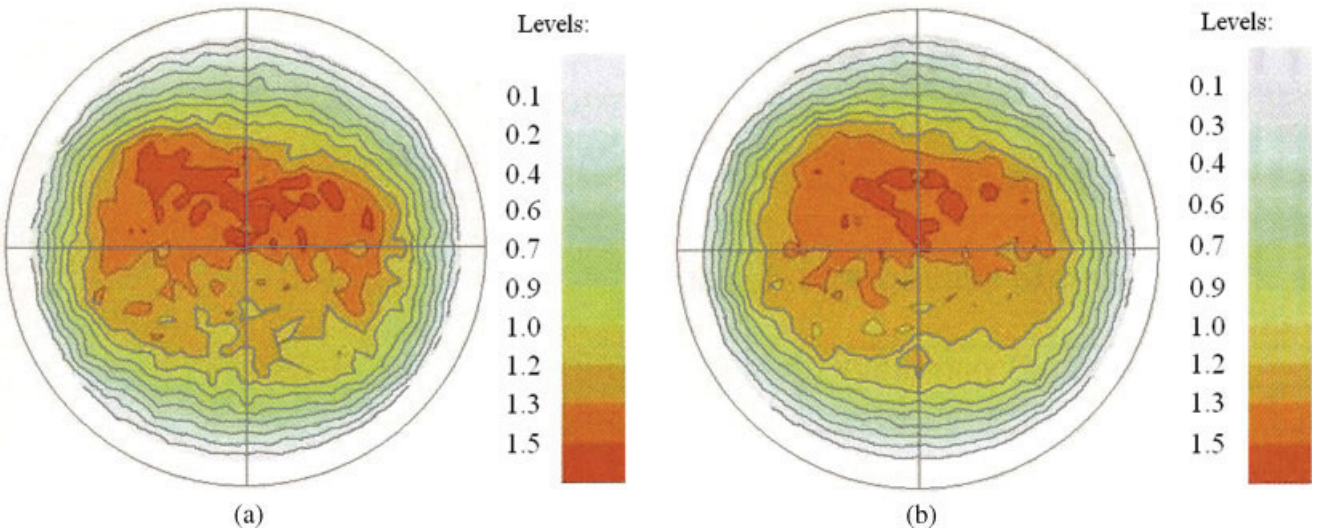

Figure 3 Pole figures of compression-molded PET. The poles correspond to (a) $2\theta = 23.1^\circ$ and (b) $2\theta = 26.2^\circ$. [Color figure can be viewed in the online issue, which is available at www.interscience.wiley.com.]

For extrudates drawn above T_g (80–100°C) and at 10 mm/min, the diffraction pattern did not change significantly from that of the as-extruded sample [Fig. 2(d,e)]. The phenomenon can be attributed to flow drawing. When the drawing temperature is above a critical value and the strain rate is relatively low, the intermolecular linkages are broken down, and the polymer molecules can slip past one another and flow individually. Under this condition, molecular relaxation processes predominate over the orientation process. Consequently, the polymer can exhibit large deformation without inducing any molecular orientation and crystallization.[16–20] When the drawing speed was increased to 1000 mm/min, three peaks appeared in the diffraction pattern [Fig. 2(e,f)] that were comparable to those at 17.7, 23.1, and 26.2° of the compression-molded specimen. Both heat-induced and drawing-induced crystals in PET fibers are triclinic.[5] In other words, these diffraction peaks were associated with the (010), ($\bar{1}$10), and (100), planes of the triclinic crystal, respectively. All these planes are roughly parallel with the molecules. This strongly indicates the effect of molecular orientation on the formation of drawing-induced crystals. The diffraction peaks of the solid-state-drawn samples were somehow less distinctive than those of the compression-molded sample. This was expected as the drawing temperatures were well below that for melt crystallization and diffusion was restricted. The effect of the drawing temperature can also be seen by a comparison of the diffraction patterns of extrudates drawn at the same speed (1000 mm/min) but at different temperatures [Fig. 2(b,f)]. Drawing temperatures above T_g facilitate the diffusion and enable crystals with a higher degree of perfection to be formed.

The pole figures of the various specimens are shown in Figures 3–6. For the compression-molded PET plate, the diffraction intensity contour lines appeared roughly as a series of concentric circles (Fig. 3). Although the PET plate possessed a highly crystalline structure, the maximum diffraction intensity level was low and generally wide spread. This suggests that the crystals were randomly oriented. In comparison, the diffraction intensity contour lines of the as-extruded PET were somewhat elliptical, and the major axes were roughly parallel to the transverse direction (Fig. 4). Because the analysis was performed

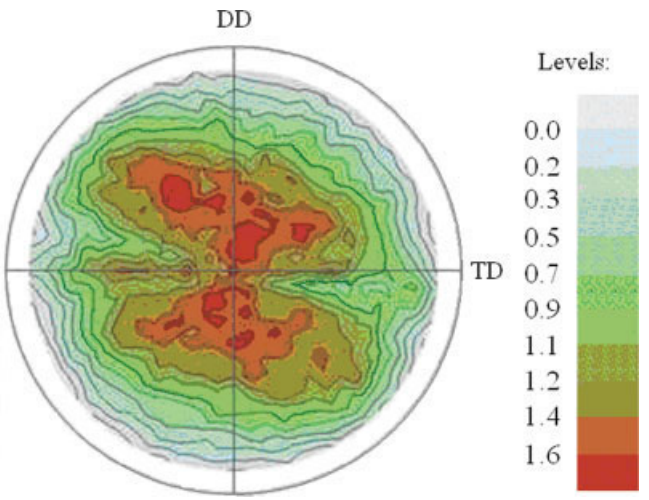

Figure 4 Pole figure of as-extruded PET. The pole corresponds to $2\theta = 22.7^\circ$ (DD = drawing direction, TD = transverse direction). [Color figure can be viewed in the online issue, which is available at www.interscience.wiley.com.]

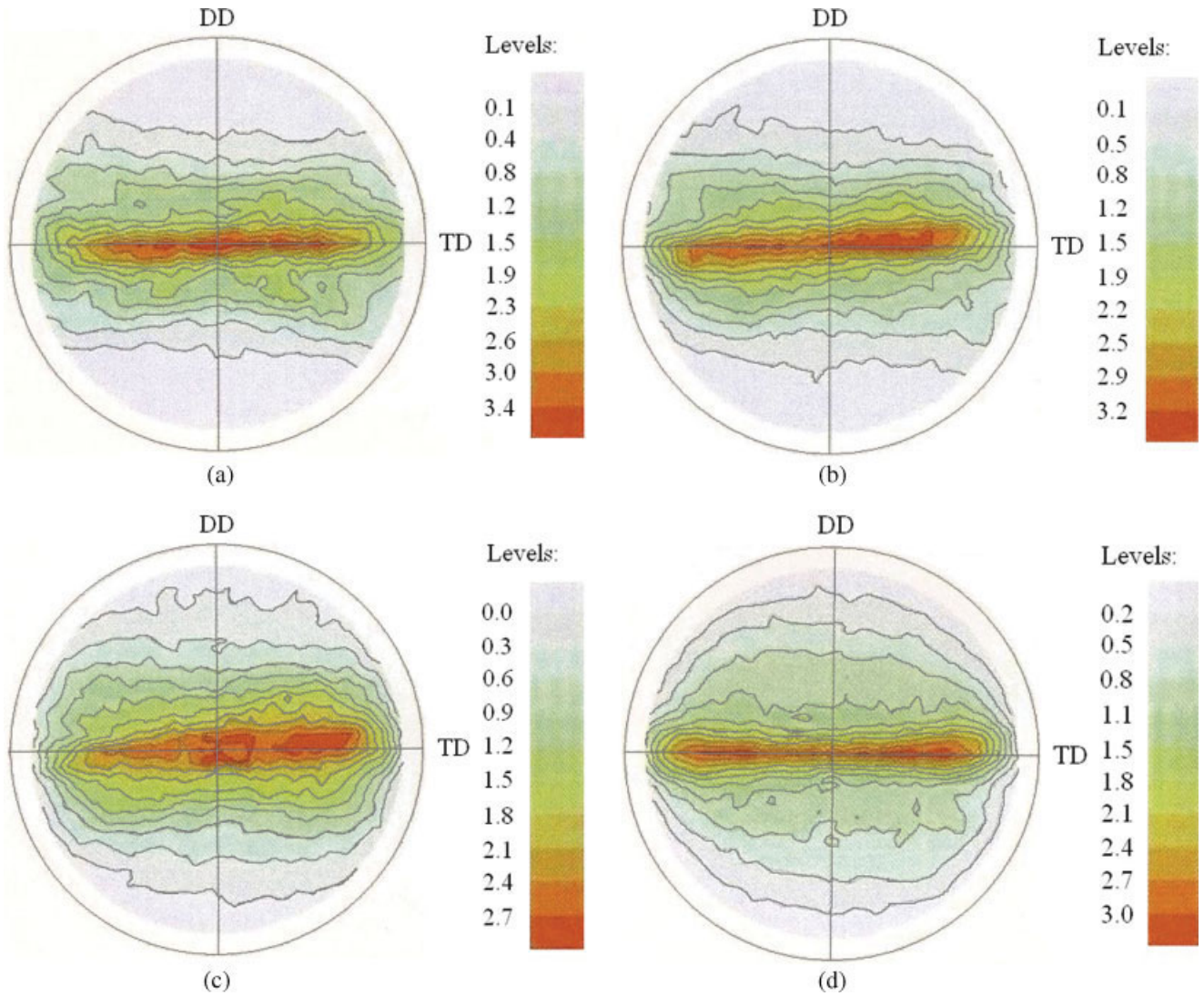

Figure 5 Pole figures of PET extrudates after drawing at 1000 mm/min and different temperatures: (a) 50, (b) 70, (c) 80, and (d) 100°C. The poles correspond to (a) $2\theta = 25.1^\circ$, (b) $2\theta = 24.9^\circ$, (c) $2\theta = 24.4^\circ$, and (d) $2\theta = 25.6^\circ$ (DD = drawing direction, TD = transverse direction). [Color figure can be viewed in the online issue, which is available at www.interscience.wiley.com.]

at $2\theta = 22.7^\circ$, which is closely associated with the $(\bar{1}10)$ pole, therefore, the result indicates a preferential alignment of the polymer molecules along the extrudates. The phenomenon can be attributed to the effect of postextrusion drawing and quenching during the extrusion process. Although the as-extruded PET had a higher molecular orientation than the molded plate, its maximum diffraction intensity was similarly low, and this was probably due to the low crystallinity. When solid-state drawing was performed at a high speed (1000 mm/min), the extrudates exhibited a strong texture of molecules aligning along the drawing direction for all the drawing temperatures up to 100°C (Fig. 5). Apparently, molecular orientation was the predominant effect over relaxation under these drawing conditions. For low-speed drawing (10 mm/min), on the other hand, a strong texture developed only in specimens drawn below T_g [Fig. 6(a–c)]. When the drawing temperature was increased to T_g and above [Fig. 6(d–f)], the strong molecular alignment gradually gave way to a more random texture. Obviously, the transition was a result of molecular relaxation. Attempts were made to study the texture of the PET microfibers; unfortunately, they became randomly oriented after xylene extraction,[2] and pole figure analysis was not possible.

Effect of annealing

Eventually, the drawn PET/PP microfibrillar composite extrudates will undergo a subsequent molding process at a temperature above the melting point of the PP matrix but below that of the PET microfibers to form the final products. In other words, the PET

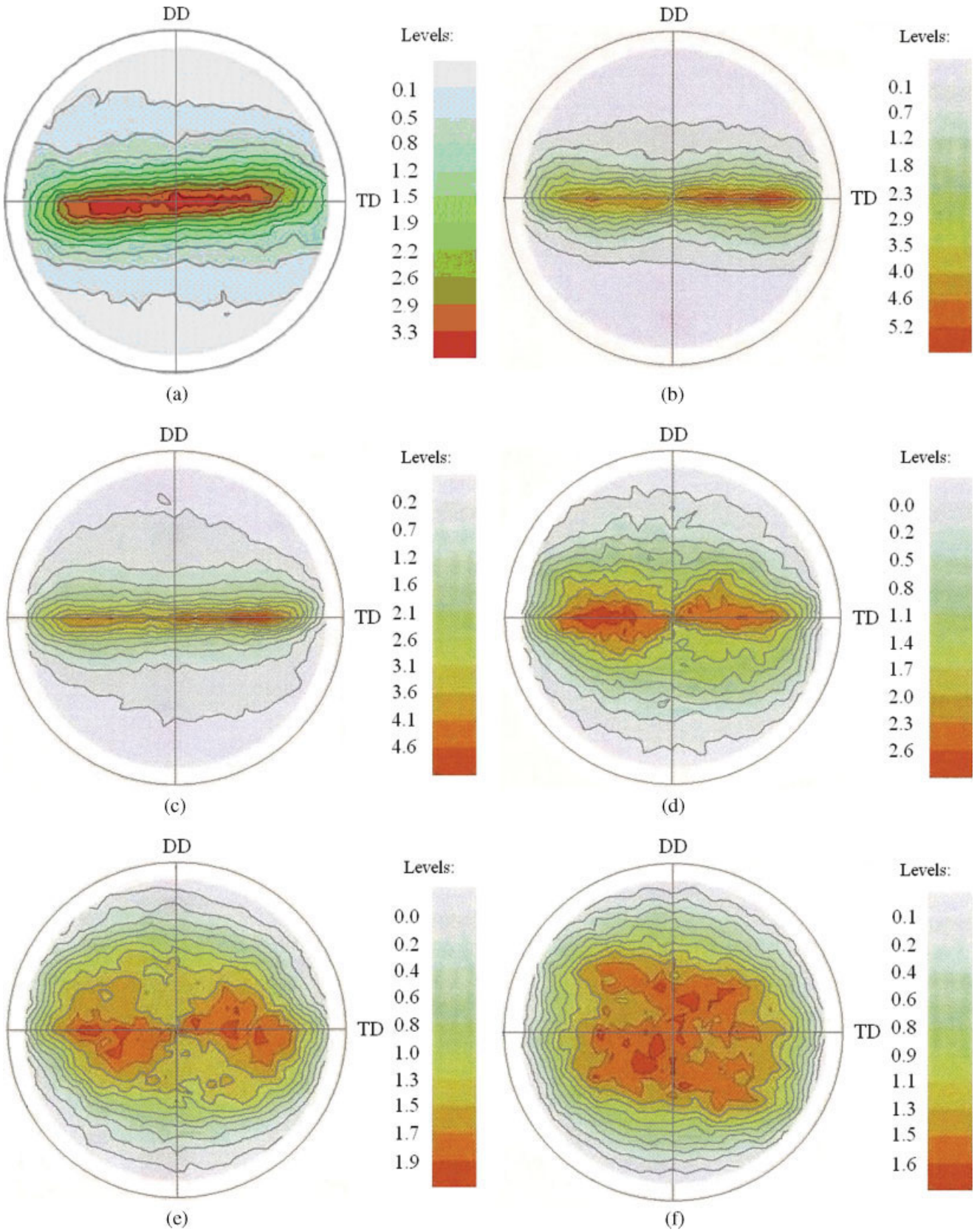

Figure 6 Pole figures of PET extrudates after drawing at 10 mm/min and different temperatures: (a) 23, (b) 50, (c) 70, (d) 80, (e) 90, and (f) 100°C. The poles correspond to (a) $2\theta = 21.8^\circ$, (b) $2\theta = 23.5^\circ$, (c) $2\theta = 24.6^\circ$, (d) $2\theta = 24.7^\circ$, (e) $2\theta = 24.0^\circ$, and (f) $2\theta = 21.0^\circ$ (DD = drawing direction, TD = transverse direction). [Color figure can be viewed in the online issue, which is available at www.interscience.wiley.com.]

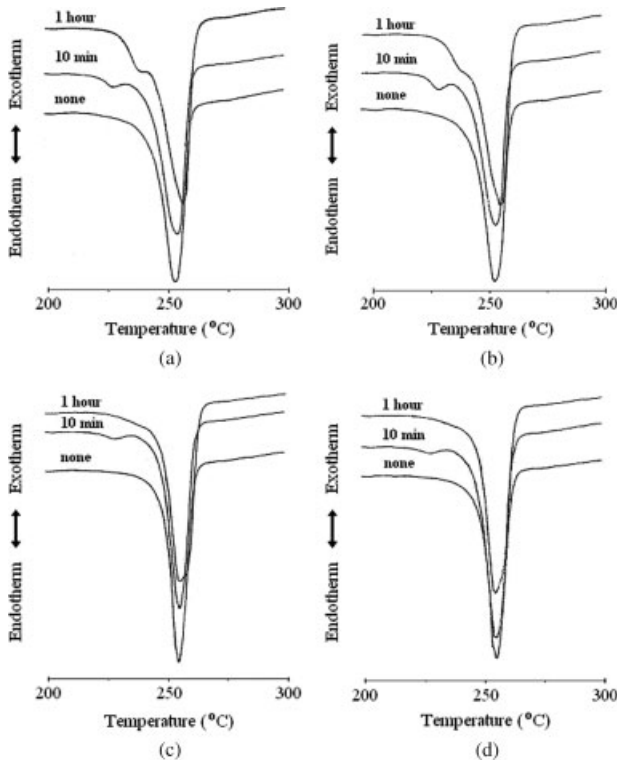

Figure 7 Effect of annealing on the fusion behavior of PET extrudates cold-drawn at different speeds: (a) 10, (b) 20, (c) 100, and (d) 200 mm/min. The annealing temperature was 220°C, and the annealing times are indicated on the curves.

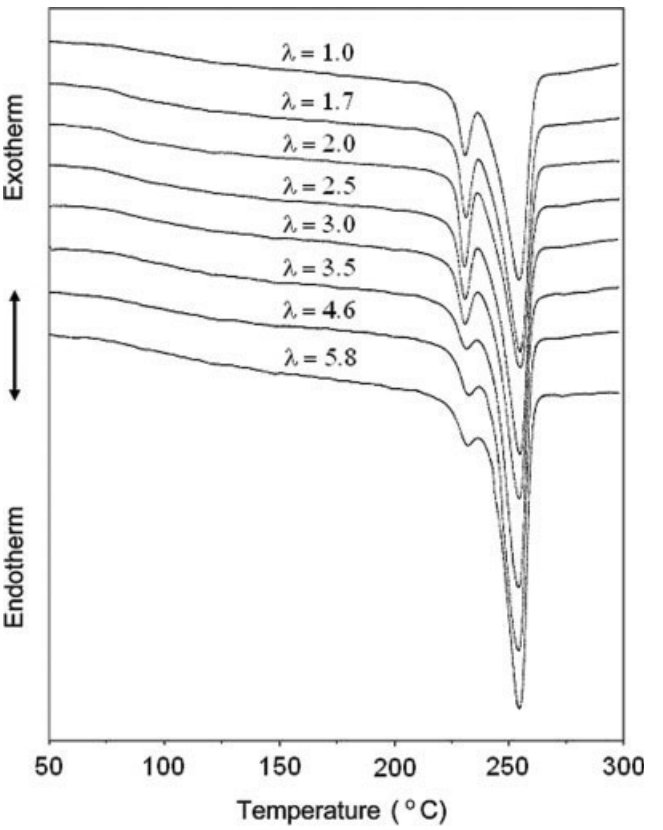

Figure 8 DSC curves of PET extrudates drawn at 100°C to different draw ratios (λ) and annealed at 220°C for 1 h.

microfibers will effectively be annealed. To simulate possible changes in the microfiber structure, annealing was conducted on some of the drawn PET extrudates, and Figures 7 and 8 show their DSC thermograms. Two endothermic peaks can be observed, and the lower peak tends to shift toward or even merge with the higher peak upon prolonged annealing, particularly for samples drawn at a higher speed or to a higher draw ratio. Multiple endothermic peaks of PET have been reported after annealing at temperatures above T_g.[21,22] The lower peak is often attributed to the melting of crystals formed in secondary crystallization, and the higher peak is often attributed to the fusion of crystals recrystallized and perfected during the DSC scan. Furthermore, the crystals formed during the primary and secondary crystallization are triclinic.[23] DSC analysis was also carried out on the extracted microfibers, and the results are shown in Figure 9. Similarly, the DSC thermograms consist of two endothermic peaks. The lower peaks were probably due to the annealing effect of the long extraction process with boiling xylene (~ 138°C).[2]

The crystallinities of the annealed extrudates and the extracted microfibers were evaluated by the integration of both endothermic peaks in Figures 7–9. For the cold-drawn extrudates and extrudates drawn at 100°C beyond the critical draw ratio for strain-induced crystallization (between draw ratios of 1.7 and 2), the crystallinity after annealing was substantially higher than that of the undrawn sample (Tables I and II). Under such drawing conditions, more molecular segments became highly oriented and were

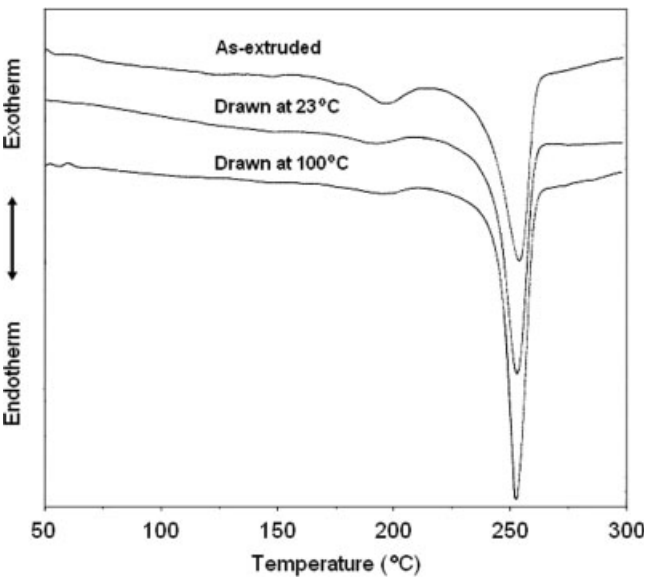

Figure 9 DSC curves of PET microfibers extracted from PET/PP extrudates drawn under different conditions.

TABLE II
Effect of Annealing (220°C) on the Crystallinity of PET Extrudates Drawn at 100°C and a Speed of 200 mm/min

Draw ratio	1	1.2	1.5	1.7	2.0	2.5	3.0	3.5	4.6	5.3	5.8
Crystallinity before annealing (%)	10.3	10.4	11.9	10.8	14.0	20.9	28.6	33.7	35.9	37.6	36.3
Crystallinity after annealing for 1 h (%)	35.2	37.3	34.0	37.7	35.6	40.8	40.2	43.8	46.7	46.6	46.3

able to crystallize during annealing. It is somewhat surprising that the crystallinity of the microfibers extracted from the cold-drawn blend was only marginally higher than that of the microfibers extracted from the as-extruded blend (Table III). One possible explanation is that they debonded from the PP matrix during cold drawing and their actual draw ratio was much lower than the overall draw ratio of the blend.[2] In comparison, the microfibers extracted from the 100°C drawn PET/PP blend showed a substantially higher crystallinity, which was more comparable to the crystallinity of the drawn PET extrudates after annealing. Therefore, the 100°C drawn blend is expected to have a slightly higher rigidity than the cold-drawn blend after subsequent molding.

All the cold-drawn extrudates exhibited a longitudinal shrinkage after annealing, and the results are listed in Table I. It has been suggested that the basic mechanism for shrinkage involves disorientation of the amorphous region.[24,25] For extrudates drawn at speeds between 20 and 200 mm/mm, the shrinkage remained more or less constant. In comparison, extrudates cold-drawn at 10 mm/min suffered a slightly lower shrinkage. The low drawing speed probably allowed a higher degree of relaxation of the molecules; hence, the extent of recovery during annealing would decrease. Apparently, 10 min was sufficient for full recovery of the stressed molecules, and further annealing to 1 h did not change the dimensions much.

Figure 10 shows the longitudinal shrinkage of PET extrudates drawn at 100°C to different draw ratios and then annealed at 220°C for 1 h. The curve can be divided into four regions: region I (draw ratio = 1–1.7), region II (draw ratio = 1.7–2.0), region III (draw ratio = 2.0–3.5), and region IV (draw ratio > 3.5). In region I, the shrinkage increases rapidly with increasing draw ratio, and the phenomenon can be attributed to the recovery of the extended molecules. It has been shown earlier[2] that there is no major change in the crystallinity within this range of draw ratios. However, there is some frozen-in strain. During the annealing process, the slightly oriented molecules return to a more random state. The phenomenon is driven by entropy. Nevertheless, the shrinkage is smaller than the draw elongation; that is, there is some translational movement between the molecules during the drawing process.

In region II, the shrinkage drops sharply from 25 to −5% (i.e., 5% elongation). Irreversible spontaneous elongation after annealing has been reported for PET samples drawn between 80 and 100°C to a draw ratio of about 2.[26] It suggests a correlation between spontaneous elongation and crystallization during annealing. Similar spontaneous elongation has also been observed in natural rubber.[27] The proposed mechanism is as follows: first, drawing causes the relative motion of molecules and produces some oriented nuclei, and second, crystallization proceeds on these nuclei, leading to a state in which the amorphous chain segments experience an axial compression and the specimen elongates. It is noteworthy that region II coincides with the critical draw ratio for strain-induced crystallization. Bundle crystallites are likely induced by drawing, and their orientation is along the fiber axis. During annealing, these crystallites act as nuclei for the crystallization of nearby molecular segments that are favorably aligned, hence resulting in a contraction in the diameter and elongation lengthwise.

In fact, the disorientation of oriented molecules and growth of strain-induced crystallites take place simultaneously during the annealing process. The overall dimensional changes of the extrudates depend on the relative extents of the two mechanisms. The latter is controlled by the number of nuclei, which in turn is controlled by the draw ratio. Before the critical draw

TABLE III
Crystallinity of PET Microfibers Extracted from As-Extruded and Solid-State-Drawn PET/PP Extrudates

Drawing condition	As-extruded	Cold-drawn at 100 mm/min	100°C drawn at 100 mm/min
Draw ratio of the extrudate	1	6.0	4.9
Crystallinity of the extracted PET fibers (%)	35.1	36.5	42.2

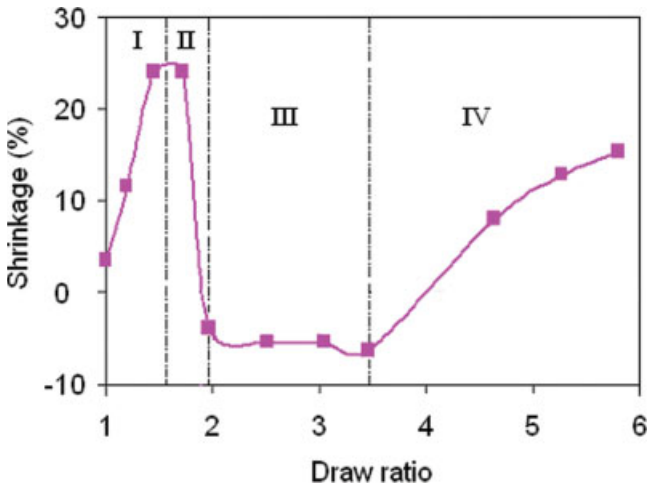

Figure 10 Effect of the draw ratio on the annealing shrinkage of PET extrudates. The extrudates were drawn at 100°C and 200 mm/min to different draw ratios before annealing at 220°C for 1 h under stress-free conditions. [Color figure can be viewed in the online issue, which is available at www.interscience.wiley.com.]

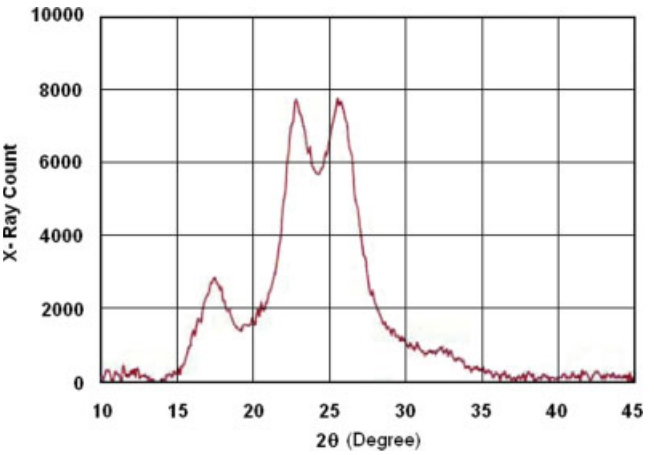

Figure 11 2θ scan pattern of PET extrudates drawn at 100°C and 1000 mm/min and then annealed at 200°C for 10 min. [Color figure can be viewed in the online issue, which is available at www.interscience.wiley.com.]

ratio, the number of nuclei is negligible, and therefore disorientation predominates. Just beyond the critical draw ratio, the number of strain-induced crystallites increases drastically. They grow during the annealing process, hence resulting in spontaneous elongation in regions II and III. In region IV, however, strain-induced crystallization consumes most of the crystallizable, amorphous material, and the extent of crystallization during annealing is greatly reduced. Disorientation of the noncrystallizable, amorphous material becomes more prevalent; therefore, shrinkage increases again. In comparison, the 100°C drawn extrudates suffered less shrinkage after annealing (Fig. 10) than the cold-drawn counterparts with similar draw ratios (Table I). For both batches, the increase in the crystallinity after annealing (for 1 h) was similar (~ 10%). The lower shrinkage of the 100°C drawn samples was probably due to less frozen-in strain before annealing.

Figure 11 shows the 2θ scan pattern of extrudates drawn at 100°C and 1000 mm/min and then annealed at 200°C for 10 min. The diffraction peaks are narrower and sharper than those before annealing [Fig. 2(f)], indicating some improvement in the degree of perfection of the crystals. Although the extrudates were annealed under stress-free conditions, the alignment of the crystals was well kept (Fig. 12). These

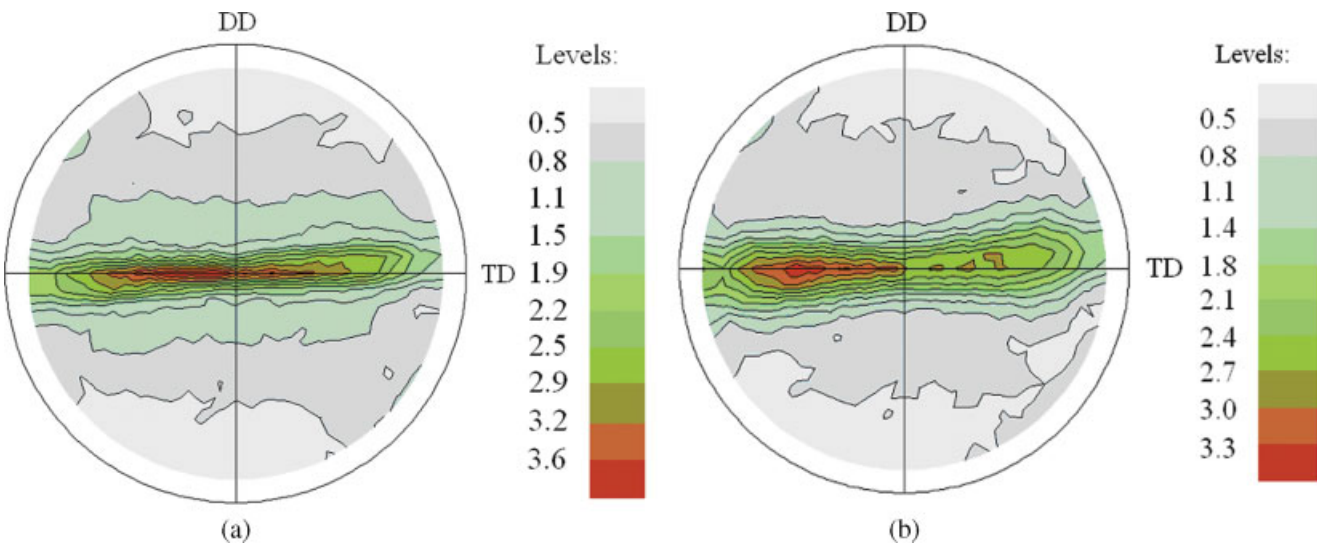

Figure 12 Pole figures of PET extrudates after drawing at 100°C and 1000 mm/min and then annealing at 200°C for 10 min. The poles correspond to (a) 2θ = 22.8° and (b) 2θ = 25.5° (DD = drawing direction, TD = transverse direction). [Color figure can be viewed in the online issue, which is available at www.interscience.wiley.com.]

results are considered to be positive signs of the preservation of the highly oriented structure and properties of the PET microfibers in the blend after subsequent molding processes.

CONCLUSIONS

The as-extruded PET had a low crystallinity of about 10% and a generally random texture. After cold drawing or drawing below T_g at a strain rate between 0.0167 and 1.67 s^{-1}, strain-induced crystallization occurred, and the crystallinity rose up to 35–37%. The strain-induced crystals were highly oriented, with a strong molecular alignment along the drawing direction; however, their structure was far from perfect. Increasing the strain rate gave a slightly more distinctive crystal structure, as reflected by the appearance of a second diffraction peak.

During drawing at temperatures above T_g, the structural development of the PET extrudates was more dependent on the strain rate. At low strain rates, the relaxation and slippage of the molecules were the major deformation mechanisms, and the extrudates were in a state of flow drawing. The texture remained more or less random, and there was little change in the crystallinity. At high strain rates, strain-induced crystallization occurred, and the crystallinity increased to a value similar to that of the cold-drawn extrudates. The more distinctive diffraction peaks suggested that thermally agitated short-range diffusion of the crystalline molecules occurred during the high-temperature drawing process.

The annealing effect on the shrinkage of the 100°C drawn extrudates was draw-ratio-dependent. Disorientation of the extended molecules was the predominant effect below the critical draw ratio. Shrinkage dropped sharply beyond the critical draw ratio, and elongation was observed between draw ratios of 2 and 3.5. The phenomenon was caused by oriented crystallization initiated by the strain-induced nuclei. A further increase in the draw ratio caused shrinkage to rise again as most crystallizable material was consumed and oriented crystallization subsided, and disorientation became more prevalent again. Annealing further increased the crystallinity of the drawn PET extrudates, but their textures were basically unchanged.

References

1. Lin, X. D.; Cheung, W. L. J Appl Polym Sci 2003, 88, 3100.
2. Lin, X. D.; Jia, D.; Leung, F. K. P.; Cheung, W. L. J Appl Polym Sci 2004, 93, 1989.
3. Koenig, J. L.; Mele, M. D. Makromol Chem 1968, 118, 128.
4. Mahendreasinggam, A.; Martin, C.; Jaber, A.; Hughes, D.; Fuller, W.; Rule, R.; Oldman, R. J.; Mackerron, D.; Blundell, D. J. Nucl Instrum Methods Phys Res Sect B 1995, 97, 238.
5. Hsieh, Y. L.; Hu, X. P. Polymer 1997, 38, 5079.
6. Bragato, G.; Gianotti, G. Eur Polym J 1983, 19, 803.
7. Cakmak, M.; White, J. L.; Spruiell, J. E. J Polym Eng 1986, 6, 291.
8. Le Bourvellec, G.; Monnerie, L.; Jarry, J. P. Polymer 1987, 28, 1712.
9. Ajji, A.; Guevremont, J.; Cole, K. C.; Dumoulin, M. M. Polymer 1996, 37, 3707.
10. Wunderlich, B. Polym Eng Sci 1978, 18, 431.
11. Astbury, W. T.; Brown, C. J. Nature 1946, 158, 871.
12. Daubeny, R. P.; Bunn, C. W. Proc R Soc London Ser A 1954, 226, 531.
13. Fakirov, S.; Fischer, E. W.; Schmidt, G. F. Makromol Chem 1975, 176, 2459.
14. Sun, T.; Zhang, A.; Li, F. M.; Porter, R. S. Polymer 1988, 29, 2115.
15. Liu, J.; Geil, P. H. J Macromol Sci 1997, 36, 61.
16. Hinrichsen, G.; Adam, H. G.; Krebs, H.; Springer, H. Colloid Polym Sci 1980, 258, 232.
17. Gupta, V. B.; Sett, S. K.; Venkataraman, A. Polym Eng Sci 1990, 30, 1252.
18. Sasano, H.; Kawai, T. Makromol Chem 1983, 184, 217.
19. Radhakrishnan, J.; Gupta, V. B. J Macromol Sci 1993, 32, 243.
20. Blundell, D. J.; Mahendrasingam, A.; Martin, C.; Fuller, W.; MacKerron, D. H.; Harvie, J. L.; Oldman, R. J.; Riekel, C. Polymer 2000, 41, 7793.
21. Zhou, C.; Clough, S. B. Polym Eng Sci 1988, 28, 65.
22. Medellin-Rodriguez, F. J.; Phillips, P. J.; Lin, J. S.; Campos, R. J Polym Sci Part B: Polym Phys 1997, 35, 1757.
23. Lin, X. D. Ph.D. Thesis, University of Hong Kong, 2000.
24. Wilson, M. P. W. Polymer 1974, 15, 277.
25. Nobbs, J. H.; Bower, D. I.; Ward, I. M. Polymer 1976, 17, 25.
26. Pereira, J. R. C.; Porter, R. S. Polymer 1984, 25, 877.
27. Bosley, D. E. J Polym Sci 1976, 20, 77.